Functional Expression of Ion Channels in Mesenchymal Stem Cells Derived from Umbilical Cord Vein

Kyoung Sun Park, Kyoung Hwa Jung, Seung Hyun Kim, Kyung Suk Kim, Mi Ran Choi, Yangmi Kim, Young Gyu Chai

STEM CELLS®

TISSUE-SPECIFIC STEM CELLS

Functional Expression of Ion Channels in Mesenchymal Stem Cells Derived from Umbilical Cord Vein

KYOUNG SUN PARK,[a] KYOUNG HWA JUNG,[a] SEUNG HYUN KIM,[b] KYUNG SUK KIM,[c] MI RAN CHOI,[c] YANGMI KIM,[d] YOUNG GYU CHAI[a]

[a]Division of Molecular and Life Science, Hanyang University, Ansan, Korea; [b]Department of Neurology, Hanyang University Hospital, Seoul, Korea; [c]Bioengineering Institute, CoreStem Inc., Seoul, Korea; [d]Department of Physiology, College of Medicine and Medical Research Institute, Chungbuk National University, Cheongju, Korea

Key Words. Mesenchymal stem cells • Voltage-gated K^+ currents • Tetrodotoxin-sensitive Na^+ current • Umbilical cord vein

ABSTRACT

Mesenchymal stem cells have the ability to renew and differentiate into various lineages of mesenchymal tissues. We used undifferentiated human mesenchymal-like stem cells from human umbilical cord vein (hUC-MSCs), a cell line which contains several mesenchymal cell markers. We characterized functional ion channels in cultured hUC-MSCs with whole-cell patch clamp and reverse transcription-polymerase chain reaction (RT-PCR). Three types of outward current were found in these cells: the Ca^{2+}-activated K^+ channel (IK_{Ca}), a transient outward K^+ current (I_{to}), and a delayed rectifier K^+ current (IK_{DR}). IK_{Ca} and IK_{DR} were totally suppressed by tetraethylammonium, and IK_{Ca} was sensitive to a specific blocker, iberiotoxin. I_{to} was inhibited by 4-aminopyridine. Another type of inward rectifier K^+ current (K_{ir}) was also detected in approximately 5% of hUC-MSCs. Elevation of external potassium ion concentration increased the K_{ir} current amplitude and positively shifted its reversal potential. In addition, inward Na^+ current (I_{Na}) was found in these cells (~30%); the current was blocked by tetrodotoxin and verapamil. In the RT-PCR analysis, Kv1.1, Kv4.2, Kv1.4, Kir2.1, heag1, MaxiK, hNE-Na, and TWIK-1 were detected. These results suggested that multiple functional ion channel currents, IK_{Ca}, IK_{DR}, I_{to}, I_{Na}, and K_{ir}, are expressed in hUC-MSCs. STEM CELLS *2007;25:2044–2052*

Disclosure of potential conflicts of interest is found at the end of this article.

INTRODUCTION

Mesenchymal stem cells in blood or tissue can differentiate into several types of cells, including adipocytes, chondrocytes, osteocytes, cardiomyocytes, and neurons [1–5]. For these reasons, MSCs have drawn considerable interest as useful materials for tissue engineering and cell-based therapy.

Human bone marrow has been recognized as one major source of MSCs for both experimental and clinical studies [1, 6–9]. However, the number of human bone marrow-derived MSCs (hBM-MSCs) and differential potential significantly decline with age [10, 11], which makes the urgency to search for adequate alternative sources of MSCs for autologous and allogeneic use necessary. Many scientists have also obtained MSCs from other sites in the adult, fetus [12], amniotic fluid [13], and BM. A few groups have also succeeded in isolating MSCs from umbilical cord (UC) blood [14–20]. Bieback et al. reported that UC blood could be an additional stem cell source for experimental and clinical purposes because MSC-like cells can be isolated at high efficacy from full-term UC blood donations [17]. The group suggested that the success rate of isolating MSCs was only 63% for UC blood. Furthermore, in a more recent report, they noted that UC blood-MSCs could be cultured longest and showed the highest proliferation capacity [18]. However, controversy still exists over whether cord blood is a source for MSCs [21, 22].

Thus, instead of using the cord blood, a potential alternative source of MSCs became possible with the culture of cells from Wharton's jelly, the primitive connective tissue of the human UC [23]. The fibroblast-like cells of human UC could be induced to differentiate into "neural-like" cells [24]. Another technical approach for human UC could be feasible to an autologous cell source of myofibroblasts for cardiovascular tissue engineering [25–28]. There are many reports on the ability of human umbilical cord (hUC)-MSCs to differentiate into several cell types of other tissues, including adipocytes, neuronal cells, chondrocytes, and osteocytes [24–26, 29–31]. hUC-MSCs could be induced to differentiate into neuron-like cells (approximately 87%) [30]. In particular, dopaminergic neurons transformed from MSCs could be transplanted into the striatum of rats previously induced to have Parkinsonism by unilateral striatal lesioning with 6-hydroxydopamine HCl [32]. These results suggest that hUC-MSCs have the potential for treatment of Parkinson disease. Also, hUC-MSCs can be induced to form cardiomyocytes by treatment with 5′-azacytidine or by culturing them in cardiomyocyte-conditioned medium [33, 34]. Many experimental reports on hUC-MSCs support the possibility that the cells might be a new source of cells for cellular therapies. Namely, hUC-MSCs are more accessible and easier to isolate compared with hBM-MSCs, and the UC can serve as a rich source of MSCs, which may be used in experimental and clinical

Correspondence: Young Gyu Chai, Ph.D., Division of Molecular and Life Science, Hanyang University, Ansan 426-791, Korea. Telephone: 82-31-400-5513; Fax: 82-31-406-6316; e-mail: ygchai@hanyang.ac.kr; or Yangmi Kim, Ph.D., Department of Physiology, College of Medicine and Medical Research Institute, Chungbuk National University, Cheongju 361-763, Korea. Telephone: 82-43-261-2861; Fax: 82-43-272-1603; e-mail: yangmik@chungbuk.ac.kr Received November 13, 2006; accepted for publication May 11, 2007; first published online in STEM CELLS *EXPRESS* May 24, 2007; available online without subscription through the open access option. 1066-5099/2007/$30.00/0 doi: 10.1634/stemcells.2006-0735

applications in treating central nervous system diseases and myocardial infarctions.

Ion channels are widely expressed in different types of cells, and they have important roles in maintaining physiological homeostasis in many cells. In the study of stem cells, there is little information about the electrophysiological properties of ion channels of human MSCs (hMSCs), although the channels may have the role as the first intracellular signal for maintaining homeostasis and differentiation [35–39]. K^+ channels are found to modulate the progression through the cell cycle in proliferating cells [40]. For therapeutic applications, we therefore have to understand not only morphological and molecular characteristics but also electrophysiological properties of ion channels in hUC-MSCs. Therefore, to begin to address this issue, we studied the population of hUC-MSCs isolated in our laboratory, and we used the whole-cell patch clamp technique to characterize the electrophysiological properties on these hUC-MSCs and reverse transcription-polymerase chain reaction (RT-PCR) to know which ion channel mRNAs are expressed.

MATERIALS AND METHODS

Isolation and Culture of hUC-MSCs

All parts of this study, especially the isolation of the human UC, were performed according to the Declaration of Helsinki. Ethical approval was obtained from Hanyang University Hospital (Seoul, Korea), and written informed consent was obtained from donors of UC. The isolation and culture of hUC-MSCs ($n = 21$) were carried out by the method previously described [25, 41]. Briefly, each UC (approximately 5 cm) was collected and processed within 6–12 hours after normal delivery. The cord vein was washed out with phosphate-buffered saline (PBS). The vessel was filled with 0.5% collagenase and incubated for 5 hours at 37°C. After gentle massage of the cord vein, the dissociated cells were collected. The cells were centrifuged for 10 minutes at 1,000 rpm and suspended in Dulbecco's modified Eagle's medium with low glucose (DMEM-LG) supplemented with penicillin-streptomycin and 10% fetal bovine serum (FBS). The cell suspension (approximately 5×10^5 cells) was seeded in 75-cm^2 culture flasks. Cultures were maintained at 37°C in a humidified atmosphere containing 5% CO_2 with a change of culture medium every other day. hBM-MSCs were purchased from Cambrex (Walkersville, MD, http://www.cambrex.com).

Flow Cytometry Analysis of hUC-MSCs

The cells were analyzed by flow cytometry (FACSCalibur A; BD Biosciences, San Diego, http://www.bdbiosciences.com). To stain the hUC-MSCs, the cells were lifted with trypsin, and the trypsin was inactivated with fresh medium. Approximately 1×10^6 cells were pelleted and resuspended in PBS and fixed with 4% buffered paraformaldehyde for 5 minutes at room temperature (21°C–24°C). For staining, nonspecific binding was blocked with PBS with 2% normal serum for 5 minutes, and then the cells were incubated with primary antibody for 45 minutes at room temperature. The cells were stained with a fluorescent secondary antibody for 30 minutes. Control cells were prepared by incubation with the secondary antibody alone. In each case, the cells were gently pelleted and washed with PBS between each incubation step. For cytoplasmic antigens, the cells were permeabilized with 100% cold methanol for 5 minutes. The following cell-surface epitopes were marked with anti-human antibodies: CD29-fluorescein isothiocyanate (FITC), CD105-FITC, HLA-DR-FITC, CD34-phycoerythrin (PE), CD45-PE (Serotec Ltd., Oxford, U.K., http://www.serotec.com), CD44-FITC, CD31-PE (DakoCytomation, Glostrup, Denmark, http://www.dakocytomation.com), CD73-PE, and CD90-PE (BD Pharmingen, San Diego, http://www.bdbiosciences.com/index_us.shtml). Mouse isotype antibodies (FITC, PE) served as a control (Serotec).

Electrophysiological Recordings

Electrophysiological recording was performed in the whole-cell configuration using a patch clamp amplifier (Axopatch 200B; Axon Instruments/Molecular Devices Corp., Union City, CA, http://www.moleculardevices.com). Borosilicate glass electrodes (1.2-mm outside diameter; Warner Instruments, Hamden, CT, http://www.warneronline.com) were pulled with a vertical pipette puller (model PP-830; Narishige, Tokyo, http://www.narishige.co.jp) and had tip resistances of 2–3 MΩ when filled with pipette solution. The tip potentials were compensated before the pipette touched the cell. After a giga-seal was obtained by negative suction, the cell membrane was ruptured by gentle suction to establish the whole-cell configuration. All recordings were performed at room temperature. The recorded signal was filtered at 2 kHz and transferred to a computer using the Digidata 1322A interface (Axon Instruments). Acquired whole cell current data were analyzed with the pCLAMP program (version 9.02; Axon Instruments).

Initially, we tried to record currents of hUC-MSCs attached to glass coverslips. However, electrophysiological recording was not feasible under these conditions. We therefore detached subconfluent hUC-MSCs from small culture flasks using trypsin-EDTA. After centrifugation at 1,000 rpm for 5 minutes, cells were recovered in culture medium. For electrophysiological recordings, the cells were transferred to a small chamber and allowed to attach to the glass bottom for 15 minutes. The suspension was stored at room temperature and used within 6 hours.

Experimental Solutions

The normal Tyrode solution contained 143 mM NaCl, 5.4 mM KCl, 0.5 mM $MgCl_2$, 1.8 mM $CaCl_2$, 0.5 mM NaH_2PO_4, 10 mM glucose, and 5 mM HEPES; the pH was adjusted to 7.4 with NaOH. The pipette solution contained 150 mM KCl, 1.0 mM $MgCl_2$, 10 mM HEPES, 5.0 mM EGTA, 2.0 mM Mg-ATP; the pH was adjusted to 7.2 with KOH. External solution was replaced by equimolar *N*-methyl-D-glucamine ($NMDG^+$) when Na^+-free conditions were applied for test of Na^+ current (I_{Na}).

Cell Culture Media, Plastics, and Chemicals

DMEM-LG, PBS, penicillin-streptomycin, trypsin-EDTA, FBS, and collagenase were obtained from Invitrogen (Carlsbad, CA, http://www.invitrogen.com). Verapamil, 4-aminopyridine (4-AP), and tetraethylammonium (TEA) were ordered from Sigma-Aldrich (St. Louis, http://www.sigmaaldrich.com), and tetrodotoxin (TTX) and iberiotoxin were from Tocris (Ellisville, MO, http://www.tocris.com).

Reverse Transcription-Polymerase Chain Reaction

Total RNA in the hUC-MSCs (after the fourth passage) was extracted using TRIzol (Invitrogen). The RNAs from hUC-MSCs were reverse transcribed to cDNA with SuperScript reverse transcriptase (Invitrogen). We resuspended 1 μg of total RNA in 25 mM deoxynucleotide triphosphate (dNTP), 1 μl of oligo(dT) (0.5 μg/ml), and 3 μl of diethylpyrocarbonate-treated water, and the suspension was subsequently heated to 65°C for 5 minutes. After cooling to 4°C, that solution was added to a mixture of 4 μl of 5X First-Strand Buffer, 2 μl of 0.1 M dithiothreitol, and 1 μl of RNase inhibitor and incubated at 42°C for 2 minutes. Then, 1 μl of SuperScript (50 units/μl) was added to the RNA solution. This was followed by incubation at 42°C for 50 minutes. Each cDNA was subjected to polymerase chain reaction (PCR) amplification using gene-specific primers. PCR was performed with 2X PCR PreMix (SolGent, Daejeon, Korea, http://www.solgent.co.kr). PCR was performed using a Promega (Madison, WI, http://www.promega.com) PCR system with *Taq* DNA polymerase and accompanying buffers. The cDNA at 2-μl aliquots was amplified by a DNA thermal cycler (Bio-Rad, Hercules, CA, http://www.bio-rad.com) in a 25-μl reaction mixture containing 1.0× thermophilic DNA polymerase reaction buffer, 1.25 mM $MgCl_2$, 0.2 mM each dNTP, 0.6 μM each forward and reverse primer, and 1.0 U of *Taq* DNA polymerase under the following conditions: the mixture was annealed at 50°C–61°C (1 minute), extended at 72°C (2 minutes), and denatured at 95°C (45 seconds) for 30–35 cycles. This was followed by a final

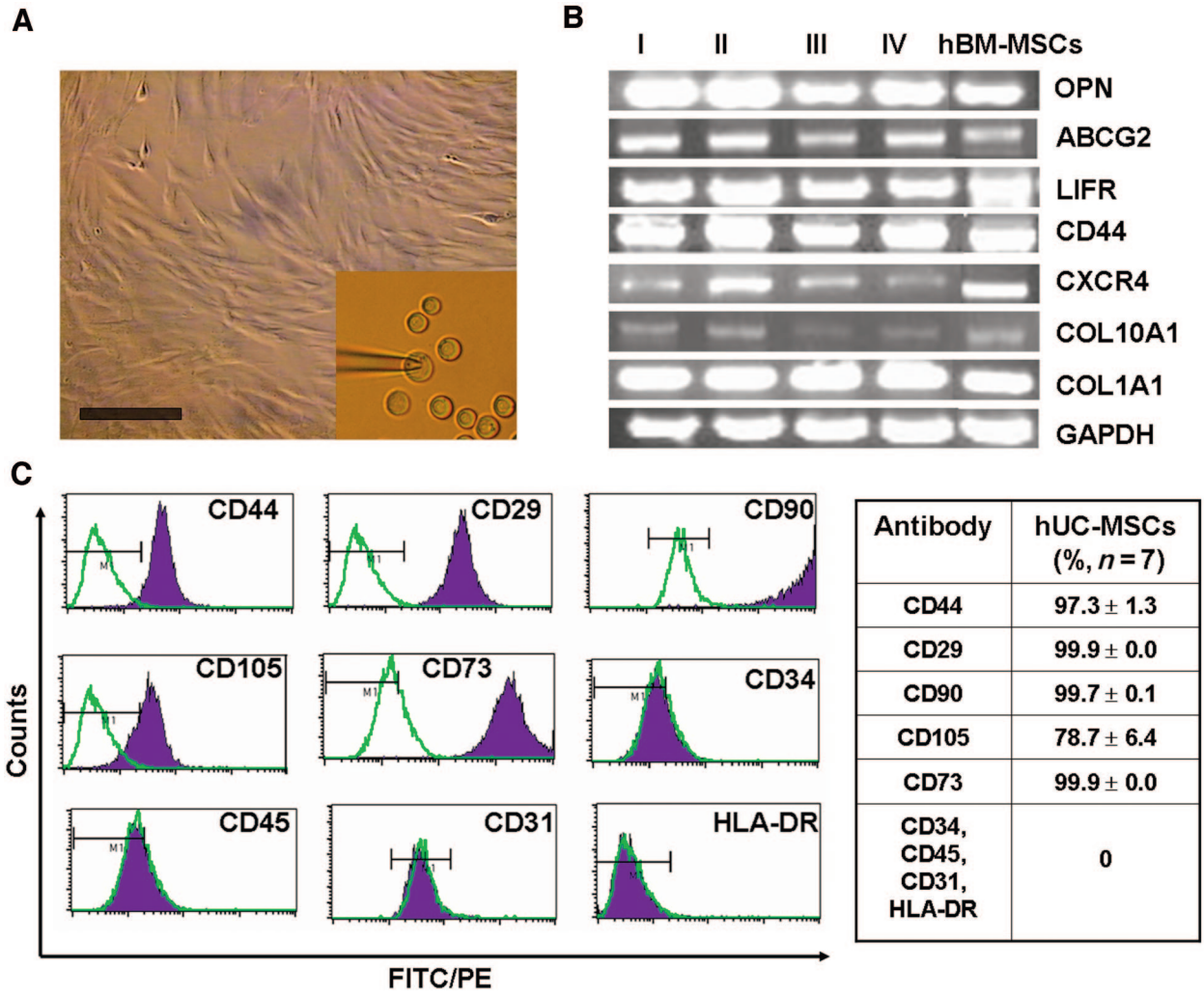

Antibody	hUC-MSCs (%, $n = 7$)
CD44	97.3 ± 1.3
CD29	99.9 ± 0.0
CD90	99.7 ± 0.1
CD105	78.7 ± 6.4
CD73	99.9 ± 0.0
CD34, CD45, CD31, HLA-DR	0

Figure 1. Characterization of hUC-MSCs. **(A):** Images showing morphology of adherent hUC-MSCs on fourth passage and ball-shaped cells after detachment from culture-flasks by trypsin-EDTA treatment and 15 minutes of attachment to the bottom of the patch-clamp chamber. The right cell was used for electrophysiological recordings (note the patch-electrode, inset). Scale bar = 50 μM. **(B):** Reverse transcription-polymerase chain reaction data compared between hUC-MSCs and human (h)BM-MSCs with the markers from reference [57]. The RNAs of hUC-MSCs were obtained from different donors (I–IV, $n = 4$) and hBM-MSCs from Cambrex. **(C):** Flow cytometry analysis showing the immunophenotype of hUC-MSCs that were obtained from the homogeneous confluent monolayer at the end of the fourth passage. The table shows mean values of the percentage of positive cells ± standard error to the total number of cells analyzed. Abbreviations: hBM-MSCs, human bone marrow-MSCs; FITC, fluorescein isothiocyanate; hUC-MSCs, human umbilical cord-MSCs; PE, phycoerythrin.

extension at 72°C (10 minutes) to ensure complete product extension. The PCR products were electrophoresed through an agarose gel, and amplified cDNA bands were visualized by ethidium bromide staining. The bands were imaged by the Gel Doc EQ System (Bio-Rad).

Data Analysis and Statistics

Nonlinear-fitting programs (OriginLab Corporation, Northampton, MA, http://www.originlab.com) were used. Results are presented as mean ± SEM. Paired and unpaired Student's t tests were used as appropriate to evaluate the statistical significance of differences between two group means. Values of $p < .05$ were considered to indicate statistical significance.

RESULTS

Characterization of Human Umbilical Cord Vein-Derived MSC Population

Human umbilical cord vein-derived mesenchymal stem cells were isolated by the previously reported procedure of Romanov et al [25]. With this approach, we regularly obtained a cell population in which we observed a spindle-shaped morphology in confluent wave-like layers in culture that was repeated 20 (or more) times. Images of cells from hUC-MSCs on the fourth passage are shown in Figure 1A. A characteristic growth pattern of a homogeneous cell phenotype was demonstrated during normal culture (data not shown). These attributes remained constant during repeated subcultivation up to the last ~10^{th} passage. Electrophysiological recordings were performed using ball-shaped cells obtained after trypsin-EDTA treatment of the cultures shown in the inset of Figure 1A. We performed an RT-PCR analysis for various genes, including markers of the undifferentiated state (LIFR, ABCG2), mesoderm markers (CXCR4, CD44, COL10A1), and extracellular matrix molecules (COL1A1) (Fig. 1B). The hUC-MSCs were obtained from different donors (lanes I–IV) and the hBM-MSCs was purchased from Cambrex. The expression levels of OPN, ABCG2, CD44, LIFR, and COL1A1 genes determined by RT-PCR were similar in the hUC-MSCs and hBM-MSCs. These cells were

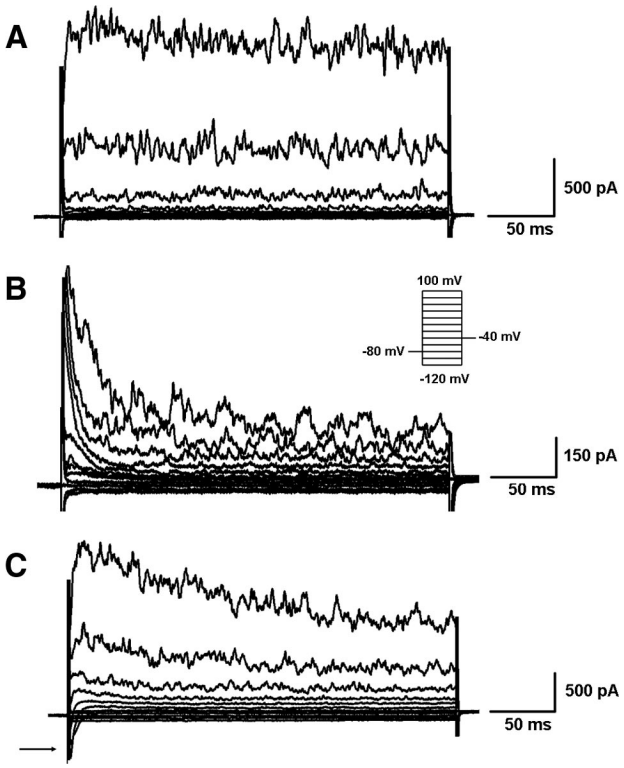

Figure 2. Different patterns of membrane currents recorded in human umbilical cord (hUC)-MSCs. **(A):** Membrane currents were activated by 300-ms voltage steps between −120 and +120 from −80 mV and then to −30 mV (as shown in the inset of **[B]**), showing that two components of outward currents are present; one is a slowly activating current similar to delayed rectifier K^+ current (IK_{DR}) at potentials from +20 to +100 mV, and the other is a rapidly activating current with noisy oscillation, similar to Ca^{2+}-activated K^+ current (IK_{Ca}) at potentials from +60 to +120 mV. **(B):** Current traces elicited by the voltage step (inset) in another hUC-MSC. The transient outward current coexisted with IK_{Ca}. **(C):** Three types of currents activated by the voltage steps (inset of **[B]**) in another hUC-MSC; an inward current was followed by IK_{DR} and IK_{Ca}. Abbreviations: ms, milliseconds; pA, picoampere.

positive for adhesion molecules (CD44), integrin markers (CD29), and extracellular matrix protein (CD90) and MSC markers (CD105, CD73) and were negative for hematopoietic (CD34, CD45), endothelial (CD31), and major histocompatibility antigen (HLA-DR) in flow cytometry analysis (Fig. 1C).

The differentiation potential of hUC-MSCs was tested by culturing under multidifferentiation conditions. Supplemental online Figure 1A–1C shows the differentiation capacity to adipocytes, osteoblasts, and chondrocytes of hUC-MSCs, respectively.

Families of Ion Channel Currents in hUC-MSCs

Membrane currents were elicited by 300-millisecond (ms) voltage steps between −120 and +100 mV from a holding potential of −80 mV in hUC-MSCs, as illustrated in Figure 2. Two types of ionic currents activated by voltage steps in hUC-MSCs are displayed in Figure 2A. One component showed a gradually activating current at potentials between +20 and +100 mV, a delayed rectifier K^+ current (IK_{DR}). Another component showed rapid activation with noisy oscillation between +60 and +120 mV. This rapidly activating component with noisy oscillation was similar to a Ca^{2+}-activated K^+ current (IK_{Ca}). We also found another type of current named a transient outward current (I_{to}) (Fig. 2B). The current was similar to the I_{to} observed in cardiac and neuronal cells, coexisting with the IK_{Ca} in other hUC-MSCs. In another experiment, we identified an inward current, followed by IK_{DR}, IK_{Ca}, and I_{to} (Fig. 2C). Most of the hUC-MSCs investigated (116 out of 125 cells, 92.8%) demonstrated IK_{DR} and IK_{Ca} currents activated by the given voltage protocols (mostly IK_{Ca} showing at over +60 mV), and I_{to} was found in more than 50% (65 out of 125 cells) of hUC-MSCs. The inward current was coexistent with outward currents in ~30% of the hUC-MSCs (36 out of 125 cells). No differences in channel type expression or ion current density were observed in the cells from different passages (ranging from third to sixth).

Characteristics of Na^+ Currents of hUC-MSCs

It is well known that an inward current such as Na^+ current or Ca^{2+} current is conducted by electrochemical driving forces in physiological solutions. Here, we found that an inward current was present in 36 out of 125 cells (~30%) in our experimental voltage protocols applied for recording outward currents (Fig. 2C). To study the nature of the inward current, we applied typical pharmacological agents such as the Na^+ channel blocker TTX and the L-type Ca^{2+} channel blocker verapamil in hUC-MSCs with inward currents. The current traces were recorded with K^+ pipette solution and normal Tyrode's bath solution with voltage steps as shown in the inset in the absence and presence of TTX (Fig. 3A). The typical inward current-voltage relationships (I-V relationships) were shown to be bell-shaped, and the current peaks were shown at 0 mV (Fig. 3A-1).

Interestingly, the inward current was blocked not only by TTX but also by verapamil (Fig. 3B). Thus, we investigated the sensitivity of two drugs on the inward current. The inward current was entirely abolished by application of TTX (100 nM) and verapamil (100 μM) in bath solution. The blocking effect on the current by TTX was recovered after a drug washout for 5 minutes, but the effect by verapamil was not fully eliminated. Half-block concentrations of TTX and verapamil on the current were 4.5 nM and 15.7 μM, respectively. To establish which ions carry the inward current, the external (bath solution) Na^+ ions were replaced by $NMDG^+$. The inward current was abolished under Na^+-free conditions in the same cell that showed effects from TTX and verapamil treatment. As shown in Figure 3B, the TTX- and verapamil-sensitive current was clearly absent in a Na^+-free bath solution (1.8 mM $CaCl_2$ remained in the bath solution). Indeed, nifedipine, L-type Ca^{2+} channel blocker, had no effect on this current (data not shown). These findings suggested that the inward current may be a TTX-sensitive I_{Na} with verapamil sensitivity.

The Existence of Inward Rectifying K^+ Currents of hUC-MSCs

We found another type of inward current in hUC-MSCs (Fig. 3C). Representative inward rectifying current traces in hUC-MSCs were evoked by a ramp voltage from −150 to +60 mV for 400 ms at 0 mV of holding potential. I-V relationships were plotted by ramp voltage-induced inward currents against membrane potentials in the bath solutions containing 5, 15, 30, 75, and 150 mM K^+ as indicated, respectively. Elevation of the external (bath solution) K^+ concentration increased the inward current amplitude and positively shifted its reversal potential after the K^+ equilibrium potential and the linear slope conductance of the inward current increased, suggesting that K^+ carries this current. I-V relationship exhibited strong inward rectification with a reversal potential of −85 mV. The currents were dose-dependently blocked by Ba^{2+} (data not shown). These properties are very similar to inward rectifier K^+ currents (K_{ir}). We conclude that K_{ir} channels are present in hUC-MSCs, where they contribute to its resting membrane potential.

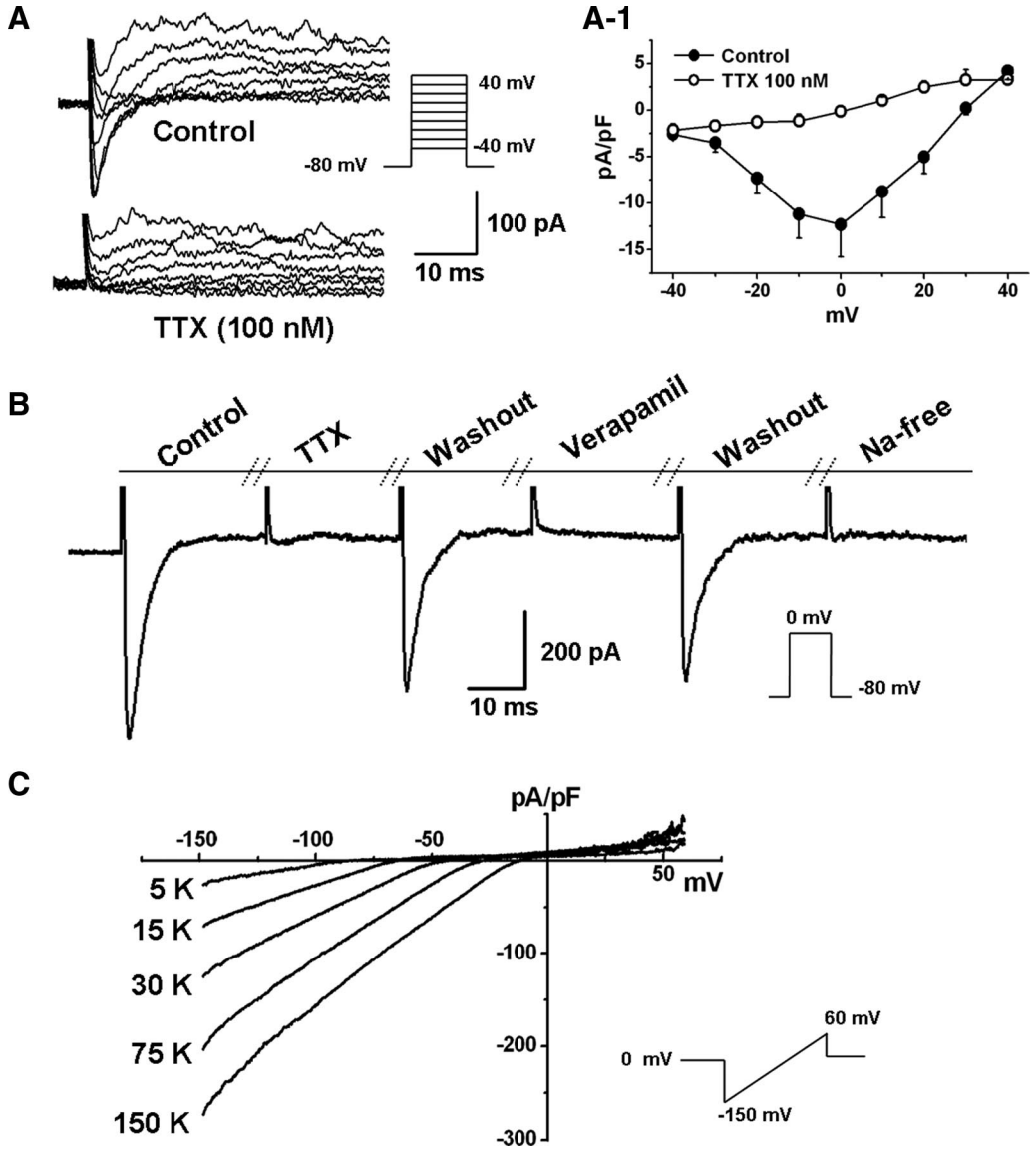

Figure 3. Two types of inward currents in human umbilical cord (hUC)-MSCs. **(A):** Current traces were recorded in hUC-MSCs with the voltage step (as shown in the inset) during control, after a 5-minute application of 100 nM TTX, and after a 5-minute drug washout. TTX reversibly abolished the inward transient without affecting the outward current. **(A-1):** Current-voltage (I-V) relationship of TTX-sensitive Na^+ currents determined in five hUC-MSCs during control (●), after the application of 100 nM TTX (○). **(B):** Time course of TTX-sensitive Na^+ currents continually recorded by 30-ms voltage step from −80 to 0 mV (as shown in the inset) in the control condition, presence of TTX, verapamil, and Na^+-free condition in the one cell of hUC-MSCs. **(C):** The I-V relationships were plotted by ramp voltage-induced inward currents against membrane potentials in the bath solutions containing 5, 15, 30, 75, and 150 mM K^+ as indicated, respectively. Representative inward current traces from a cell were evoked by a ramp voltage from −150 to +60 mV for 400 ms. Abbreviations: ms, milliseconds; Na, sodium; pA, picoampere; pF, picofarad; TTX, tetrodotoxin.

Outward K^+ Currents of hUC-MSCs

All hUC-MSCs investigated demonstrated outward currents (125 out of 125 cells). We found that three types of outward current were present in hUC-MSCs, including IK_{Ca}, IK_{DR}, and I_{to}.

The most abundant outward current rapidly activated at positive voltages. As shown in Figure 4, current traces were recorded in a representative cell with the voltage protocol shown in the inset. The noisy oscillation current was remarkably reduced by application of 100 nM iberiotoxin (Fig. 4A). This current was identified as a Ca^{2+}-activated K^+ current, conducted by big conductance K^+ (MaxiK or BK_{Ca}) channels, due to its high sensitivity to iberiotoxin, which is known as a MaxiK channel-specific blocker. The remaining current detected with the voltage protocol shown in the inset was inhibited by TEA in a dose-dependent manner (Fig. 4B), suggesting that IK_{Ca} was coexistent with IK_{DR} in hUC-MSCs.

I_{to} traces recorded in representative hUC-MSCs under control conditions and after the application of 4-AP and TEA are shown in Figure 5A. I_{to} was substantially inhibited by 300 μM 4-AP, whereas TEA had no effect on it. I_{to} at +60 mV was inhibited to 8.8 ± 4.2 picoampere (pA)/picofarad (pF) from 26.4 ± 4.7 pA/pF of the control ($n = 6$). I-V relationships of I_{to} mean values in the absence and presence of 4-AP are displayed in Figure 5A-1. The inhibition was relieved after washout of the drug for less than 5 minutes.

The percentages of hUC-MSCs expressing ion channel patterns are summarized in Figure 5C. Because almost all patch samples showed the TEA-sensitive current (IK_{TEA}), we

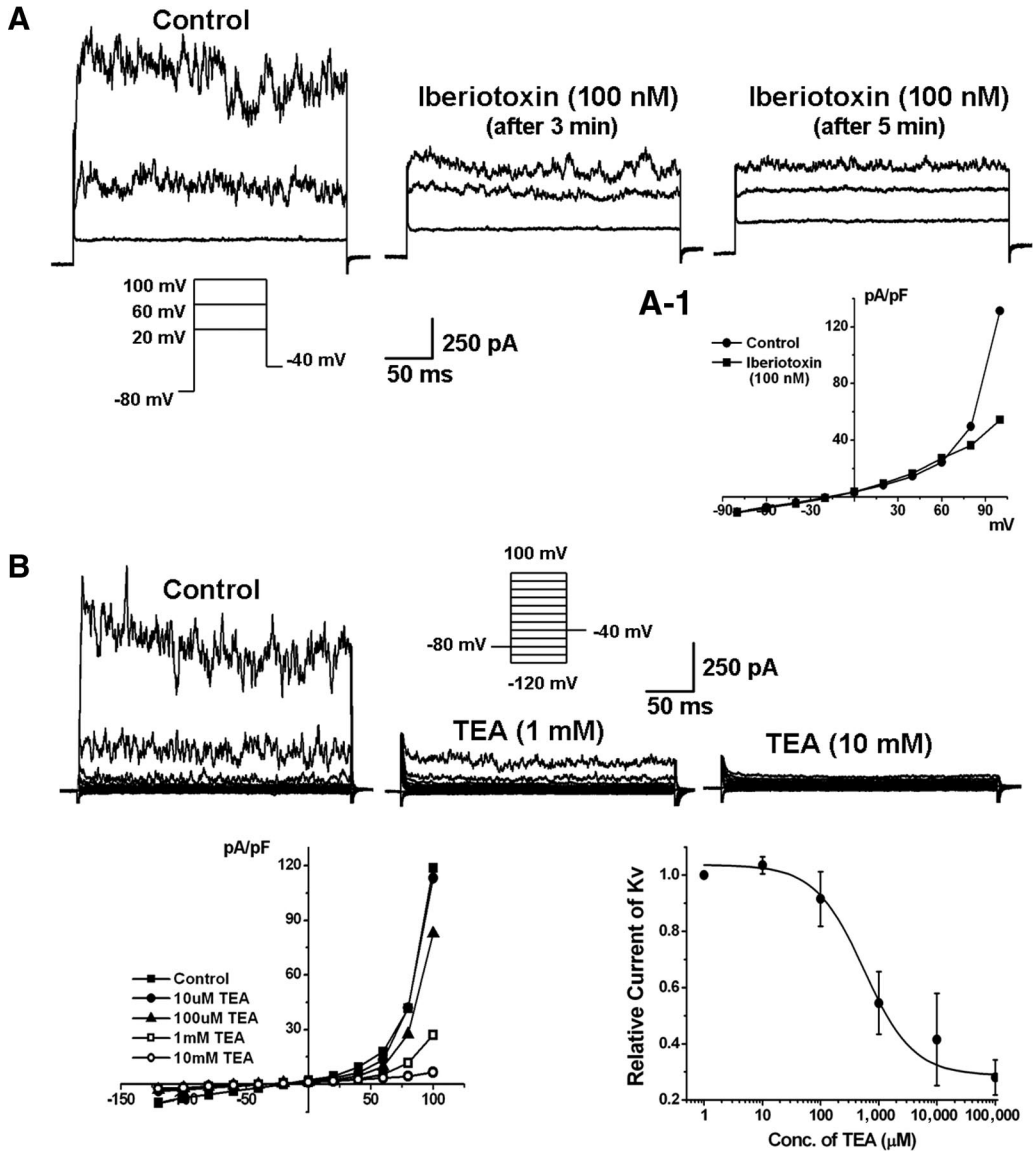

Figure 4. Iberiotoxin- and TEA-sensitive K^+ currents in human umbilical cord (hUC)-MSCs. **(A):** Membrane currents were recorded with the 300-ms voltage steps as shown in the inset in the absence (control) and presence of 100 nM iberiotoxin (a blocker of Ca^{2+}-activated K^+ current [IK_{Ca}]). **(A-1):** Current-voltage (I-V) relationship of iberiotoxin-sensitive currents determined in the control (●) after the application of 100 nM iberiotoxin (■). **(B):** Membrane currents were recorded with the 300-ms voltage steps as shown in the inset in the absence (control) and presence of 1 mM TEA (a blocker of IK_{Ca} and human ether a go-go K^+ current) and 10 mM TEA (upper panel). I-V relationships of currents in the control (■), 10 μM TEA (●), 100 μM TEA (▲), 1 mM TEA (□), and 10 mM TEA (○). TEA substantially inhibited the K^+ current at test potentials from +20 mV to +100 mV (lower-left panel). Dose-dependent effects of TEA on hUC-MSCs at +100 mV were plotted (lower-right panel, $n = 5$ cells per concentration). Abbreviations: min, minutes; ms, milliseconds; pA, picoampere; pF, picofarad; TEA, tetraethylammonium.

set the expression rate of IK_{TEA} to 100% and then measured the expression rate of I_{to}, I_{Na}, and K_{ir} comparatively. Ion channel expression rates were 52% (65 of 125), 28.8% (63 of 125), and 4.8% (6 of 125) in I_{to}, I_{Na}, and K_{ir}, respectively.

mRNA Expression of Functional Ion Channels in hUC-MSCs

To study the molecular identity of the functional ionic currents observed, we investigated the expression pattern in hUC-MSCs with RT-PCR using specific primers (Fig. 6B). Figure 6A displays the mRNA expression (mRNA) for ion channel α-subunits related to functional outward and inward ionic currents. High mRNA levels of MaxiK (responsible for IK_{Ca}), Kv1.4 and Kv4.2 (responsible for I_{to}), Kv1.1 and heag1 (responsible for IK_{DR}), hNE-Na (responsible for I_{Na}), and Kir2.1 (responsible for K_{ir}) were detected in hUC-MSCs. We used β-actin for the control. These results provide the molecular basis for the functional ionic currents observed in hUC-MSCs.

DISCUSSION

In this report, we have demonstrated that several specialized K^+ channels and Na^+ channels at the mRNA and functional levels were present in undifferentiated human MSCs from the umbilical cord vein. The direct comparison reported here showed that hUC-MSCs and hBM-MSCs express the same gene markers (Fig. 1B) and share common cell surface antigens (Fig. 1C). Also, hUC-MSCs have an ability to undergo multilineage mesenchymal differentiation (supplemental online Fig. 1). Ca^{2+}-

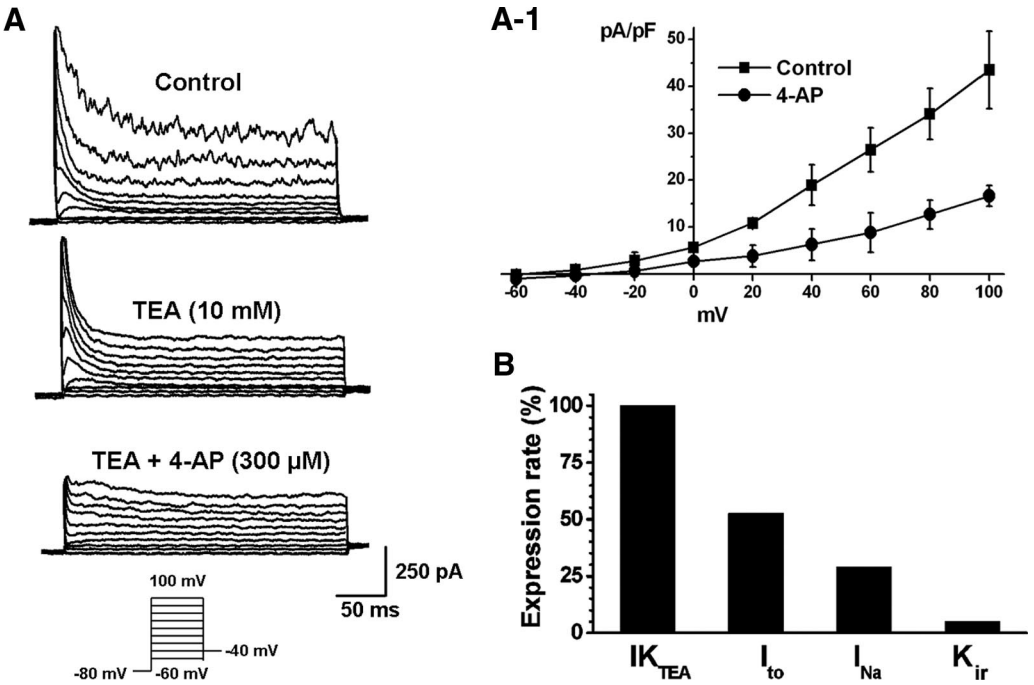

Figure 5. Transient outward K^+ currents and comparison of each channel in human umbilical cord (hUC)-MSCs. **(A):** Membrane currents were recorded with the 300-ms voltage steps as shown in the inset in the absence (control) and presence of 10 mM TEA and coapplication of TEA and 300 μM 4-AP (a blocker of I_{to}). **(A-1):** Current-voltage relationship of I_{to} in the control (■) after the application of 300 μM 4-AP (●). **(B):** Comparison of IK_{TEA}, I_{to}, I_{Na}, and K_{ir} in hUC-MSCs. IK_{TEA} was recorded from nearly all (~95%) cells. We set the expression rate of IK_{TEA} at 100%, and then the expression rates of I_{to}, I_{Na}, and K_{ir} were measured comparatively. Abbreviations: 4-AP, 4-aminopyridine; IK_{TEA}, tetraethylammonium-sensitive current; I_{Na}, Na^+ current; I_{to}, transient outward current; K_{ir}, inward rectifier K^+ current; ms, milliseconds; pA, picoampere; pF, picofarad; TEA, tetraethylammonium.

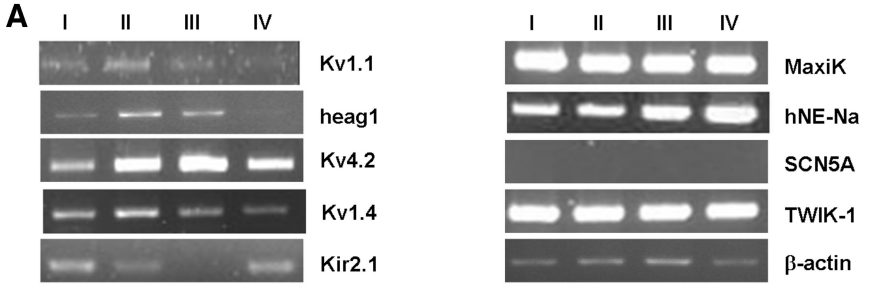

B

Gene	Acc. No.	Forward primer (5'-3')	Reverse primer (5'-3')	bp
Kv1.1	L02750	CCATCATTCCTTATTTCATCAC	CTCTTCCCCCTCAGTTTCTC	488
heag1	AJ001366	TGGATTTTGCAAGCTGTCTG	GAGTCTTTGGTGCCTCTTGC	476
Kv4.2	AJ010969	ATCTTCCGCCACATCCTGAA	GATCCGCACGGCACTGTTTC	362
Kv1.4	L02751	GAGAGAAGAGGAAGACAGGGC	TGGGGTGCTGAAGTATCATTC	246
Kir2.1	L36069	GACCTGGAGACGGACGAC	AGCCTGGAGTCTGTCAAAGTC	393
MaxiK	U11058	ACAACATCTCCCCCAACC	TCATCACCTTCTTTCCAATTC	385
hNE-Na	X82835	GCTCCGAGTCTTCAAGTTGG	GGTTGTTTGCATCAGGGTCT	446
SCN5A	M77235	CCTAATCATCTTCCGCATCC	TGTTCATCTCTCTGTCCTCATC	208
Twik1	U336321	TCCTGCTTCTTCTTCATC	AGGCTCATTTTGCTTCTGGTC	385
β-actin	NM001101	TCATGTTTGAGACCTTCAA	GTCTTTGCGGATGTCCACG	512

Figure 6. mRNA expression of ion channel subunits related to the functional ionic currents was amplified by reverse transcription-polymerase chain reaction (RT-PCR). List of primers used is given. **(A):** Original gel showing significant levels of Kv1.1, heag1, Kv4.2, Kv1.4, Kir2.1, MaxiK, hNE-Na, SCN5A, and TWIK-1 (housekeeping gene: β-actin). RNAs of human umbilical cord-MSCs were obtained from different donors ($n = 4$). **(B):** List of primers used for RT-PCR. Abbreviations: Acc. No., accession number; bp, base pairs.

activated K^+ channel, delayed rectifying K^+ current, and transient outward K^+ current were present mainly in hUC-MSCs, although inward rectifying K^+ current and Na^+ current were present in a small portion of the population. Also, we demonstrated characteristics of hUC-MSCs with morphological and immunophenotypical methods. To our knowledge, this is the

first time that hUC-MSCs have been extensively characterized from an electrophysiological viewpoint, not just in hBM-MSCs as studied until now [8, 9, 42].

Characteristics and Functional Role of Ion Channels in hUC-MSCs

Electrophysiologically isolated IK_{DR} and I_{to} from hUC-MSCs were confirmed as *Kv1.1*, *heag1*, *Kv4.2*, and *Kv1.4* by RT-PCR. The Kv1.1 subfamily is expressed in the embryonic nervous system [43, 44], and mutations in Kv1.1 are associated with human episodic ataxia type 1 syndrome, which is characterized by movement disorders and epilepsy [45, 46]. Mammalian ether a go-go (EAG) subfamily K^+ channels have been studied in several species including rat [47], mouse [48], bovine [49], and human [50]. Human EAG (heag) K^+ channels were found to participate in cell proliferation in human breast cancer cells, and inhibition of heag K^+ channels arrested cells in the early G1 phase [39].

I_{to} was first observed in hMSCs through mRNA expression analysis by Heubach et al. [9], and then it was detected in a small population of hMSCs (~8%) by another group [8]. However, in our group, surprisingly, I_{to} was recorded in over 50% of hUC-MSCs. During development of embryonic stem cell-derived cardiomyocytes, inhibition of I_{to} by 4-AP changed the duration and frequency of action potentials in the early stage but not in the late stage, suggesting that the I_{to} of early-stage cardiomyocytes plays an important role in controlling electrical activity [51]. These reports suggest that K^+ currents may modulate progression through the cell cycle in proliferating cells and in early embryonic development as well as at later stages of differentiation [37, 38, 40, 52].

IK_{Ca} usually coexists with IK_{DR}, and the channel was proven to have a MaxiK channel by pharmacological and molecular biological approaches (Figs. 4, 6). MaxiK channels are usually believed to be sensors of intracellular Ca^{2+} and are found to regulate membrane potential in an intracellular Ca^{2+}-dependent manner in hMSCs [36]. These results suggest that MaxiK current could, therefore, be an effector of trophic factors within the body fluids or cell culture medium.

Voltage-gated Na^+ channels are responsible for action potential initiation and propagation in excitable cells, including nerve, muscle, and neuroendocrine cells. We recorded I_{Na} in about 30% of hUC-MSCs and found that the current was highly sensitive to blockage by TTX (Fig. 3A). $Na_V1.7$ (SCN9A or hNE-Na) is highly TTX sensitive and is broadly expressed in neurons, whereas $Na_V1.5$ (SCN5A) is TTX resistant [53]. Electrophysiological properties and mRNA expression pattern of Na^+ channel of hUC-MSCs are consistent with the report by Li et al [42]. Unexpectedly, TTX-sensitive Na^+ current in hUC-MSCs was also inhibited by verapamil, known as an L-type Ca^{2+} channel-specific blocker. Furthermore, the current was not eliminated in the absence of Ca^{2+}, and Ca^{2+} channel transcripts (*1αC*, *1αD*, *1αG*, *1αH*, and *1αS*) were not detected by RT-PCR analysis (data not shown). However, some groups observed the L-type Ca^{2+} channel in hBM-MSCs using patch clamp and RT-PCR analysis [8, 9]. These results suggest that the variety of ion channel distribution in MSCs may depend on the species or source of MSCs. Na^+ channel may play important physiological roles during differentiation of hUC-MSCs into cardiac cells and neuronal cells. Therefore, further studies on the late passages or differentiated cells are needed because these characteristics of the channel may disappear during differentiation of hMSCs. In our view, undifferentiated cells may have undifferentiated channels.

We also demonstrated the presence of an inwardly rectifying K^+ current in a small population of hUC-MSCs. *Kir2.1* (classic K_{ir} channel or IRK1) transcript was detected by RT-PCR. To our knowledge, this is the first electrophysiological recording of K_{ir} in human MSCs, not in rodent MSCs [42, 54]. Usually K_{ir} likely plays a dominant role in the maintenance of resting membrane potential, in regulating the action potential duration, and thus in controlling the excitability of a variety of cells. It has been reported that K_{ir} is distributed in hemopoietic progenitor cells and neural stem cells [55, 56], raising the possibility that the presence of K_{ir} might be a physiological marker for the pluripotent neural stem cells or neural progenitor cells.

Functional Implications and Conclusions

The present observations focused on the functional expression of ion channels, and we demonstrated that various ion channels are present in hUC-MSCs. An understanding of the regulation of ion channels in undifferentiated hUC-MSCs will be helpful to investigate possible biological solutions, such as gene and/or cell therapy, to medical challenges such as teratogenicity, infection, and immune rejection. Our results provide strong support for the study of the physiological roles of these ionic currents in the proliferation and differentiation of hMSCs in the future, in order to gather more information on human stem cell biology.

ACKNOWLEDGMENTS

This work was supported by a Grant (034475) from the BioGreen 21 Program, Rural Development Administration, a Grant (KOSEF-2006-04670) from the Basic Research Program of the Korea Science & Engineering Foundation (KOSEF), and a Grant from Korea Research Foundation (R05-2004-000-11589-0). K.S.P. and K.H.J. equally contributed as first author.

DISCLOSURE OF POTENTIAL CONFLICTS OF INTEREST

The authors indicate no potential conflicts of interest.

REFERENCES

1 Pittenger MF, Mackay AM, Beck SC et al. Multilineage potential of adult human mesenchymal stem cells. Science 1999;284:143–147.
2 Sanchez-Ramos J, Song S, Cardozo-Pelaez F et al. Adult bone marrow stromal cells differentiate into neural cells in vitro. Exp Neurol 2000; 164:247–256.
3 Deans RJ, Moseley AB. Mesenchymal stem cells: Biology and potential clinical uses. Exp Hematol 2000;28:875–884.
4 Negishi Y, Kudo A, Obinata A et al. Multipotency of a bone marrow stromal cell line, TBR31–2, established from ts-SV40 T antigen gene transgenic mice. Biochem Biophys Res Commun 2000;268:450–455.
5 Forbes SJ, Vig P, Poulsom R et al. Adult stem cell plasticity: New pathways of tissue regeneration become visible. Clin Sci (Lond) 2002; 103:355–369.
6 Theise ND, Nimmakayalu M, Gardner R et al. Liver from bone marrow in humans. Hepatology 2000;32:11–16.
7 Orlic D, Kajstura J, Chimenti S et al. Bone marrow cells regenerate infarcted myocardium. Nature 2001;410:701–705.
8 Li GR, Sun H, Deng X et al. Characterization of ionic currents in human mesenchymal stem cells from bone marrow. STEM CELLS 2005;23:371–382.
9 Heubach JF, Graf EM, Leutheuser J et al. Electrophysiological properties of human mesenchymal stem cells. J Physiol 2004;554:659–672.
10 Rao MS, Mattson MP. Stem cells and aging: Expanding the possibilities. Mech Ageing Dev 2001;122:713–734.
11 Mueller SM, Glowacki J. Age-related decline in the osteogenic potential of human bone marrow cells cultured in three-dimensional collagen sponges. J Cell Biochem 2001;82:583–590.

12 In 't Anker PS, Noort WA, Scherjon SA et al. Mesenchymal stem cells in human second-trimester bone marrow, liver, lung, and spleen exhibit a similar immunophenotype but a heterogeneous multilineage differentiation potential. Haematologica 2003;88:845–852.
13 In 't Anker PS, Scherjon SA, Kleijburg-van der Keur C et al. Amniotic fluid as a novel source of mesenchymal stem cells for therapeutic transplantation. Blood 2003;102:1548–1549.
14 Goodwin HS, Bicknese AR, Chien SN et al. Multilineage differentiation activity by cells isolated from umbilical cord blood: Expression of bone, fat, and neural markers. Biol Blood Marrow Transplant 2001;7:581–588.
15 Rosada C, Justesen J, Melsvik D et al. The human umbilical cord blood: A potential source for osteoblast progenitor cells. Calcif Tissue Int 2003;72:135–142.
16 Feldmann RE Jr., Bieback K, Maurer MH et al. Stem cell proteomes: A profile of human mesenchymal stem cells derived from umbilical cord blood. Electrophoresis 2005;26:2749–2758.
17 Bieback K, Kern S, Kluter H et al. Critical parameters for the isolation of mesenchymal stem cells from umbilical cord blood. STEM CELLS 2004;22:625–634.
18 Kern S, Eichler H, Stoeve J et al. Comparative analysis of mesenchymal stem cells from bone marrow, umbilical cord blood, or adipose tissue. STEM CELLS 2006;24:1294–1301.
19 Lee OK, Kuo TK, Chen WM et al. Isolation of multipotent mesenchymal stem cells from umbilical cord blood. Blood 2004;103:1669–1675.
20 Erices A, Conget P, Minguell JJ. Mesenchymal progenitor cells in human umbilical cord blood. Br J Haematol 2000;109:235–242.
21 Mareschi K, Biasin E, Piacibello W et al. Isolation of human mesenchymal stem cells: Bone marrow versus umbilical cord blood. Haematologica 2001;86:1099–1100.
22 Wexler SA DC, Denning-Kendall P, Rice C et al. Adult bone marrow is a rich source of human mesenchymal 'stem' cells but umbilical cord and mobilized adult blood are not. Br J Haematol 2003;121:368–374.
23 McElreavey KD, Irvine AI, Ennis KT et al. Isolation, culture and characterisation of fibroblast-like cells derived from the Wharton's jelly portion of human umbilical cord. Biochem Soc Trans 1991;19:29S.
24 Mitchell KE, Weiss ML, Mitchell BM et al. Matrix cells from Wharton's jelly form neurons and glia. STEM CELLS 2003;21:50–60.
25 Romanov YA, Svintsitskaya VA, Smirnov VN. Searching for alternative sources of postnatal human mesenchymal stem cells: Candidate MSC-like cells from umbilical cord. STEM CELLS 2003;21:105–110.
26 Covas DT, Siufi JL, Silva AR et al. Isolation and culture of umbilical vein mesenchymal stem cells. Braz J Med Biol Res 2003;36:1179–1183.
27 Kadner A, Hoerstrup SP, Tracy J et al. Human umbilical cord cells: A new cell source for cardiovascular tissue engineering. Ann Thorac Surg 2002;74:S1422–S1428.
28 Kadner A, Zund G, Maurus C et al. Human umbilical cord cells for cardiovascular tissue engineering: A comparative study. Eur J Cardiothorac Surg 2004;25:635–641.
29 Kim JW, Kim SY, Park SY et al. Mesenchymal progenitor cells in the human umbilical cord. Ann Hematol 2004;83:733–738.
30 Fu YS, Shih YT, Cheng YC et al. Transformation of human umbilical mesenchymal cells into neurons in vitro. J Biomed Sci 2004;11:652–660.
31 Baksh D, Yao R, Tuan RS. Comparison of proliferative and multilineage differentiation potential of human mesenchymal stem cells derived from umbilical cord and bone marrow. STEM CELLS 2007;25:1384–1392.
32 Fu YS, Cheng YC, Lin MY et al. Conversion of human umbilical cord mesenchymal stem cells in Wharton's jelly to dopaminergic neurons in vitro: Potential therapeutic application for Parkinsonism. STEM CELLS 2006;24:115–124.
33 Wang HS, Hung SC, Peng ST et al. Mesenchymal stem cells in the Wharton's jelly of the human umbilical cord. STEM CELLS 2004;22:1330–1337.
34 Kadivar M, Khatami S, Mortazavi Y et al. In vitro cardiomyogenic potential of human umbilical vein-derived mesenchymal stem cells. Biochem Biophys Res Commun 2006;340:639–647.
35 Kawano S, Shoji S, Ichinose S et al. Characterization of Ca^{2+} signaling pathways in human mesenchymal stem cells. Cell Calcium 2002;32:165–174.
36 Kawano S, Otsu K, Shoji S et al. Ca^{2+} oscillations regulated by Na^{+}-Ca^{2+} exchanger and plasma membrane Ca^{2+} pump induce fluctuations of membrane currents and potentials in human mesenchymal stem cells. Cell Calcium 2003;34:145–156.
37 Day ML, Pickering SJ, Johnson MH et al. Cell-cycle control of a large-conductance K^{+} channel in mouse early embryos. Nature 1993;365:560–562.
38 Patil N, Cox DR, Bhat D et al. A potassium channel mutation in weaver mice implicates membrane excitability in granule cell differentiation. Nat Genet 1995;11:126–129.
39 Ouadid-Ahidouch H, Le Bourhis X, Roudbaraki M et al. Changes in the K^{+} current-density of MCF-7 cells during progression through the cell cycle: Possible involvement of a h-ether.a-gogo K^{+} channel. Receptors Channels 2001;7:345–356.
40 Wonderlin WF, Strobl JS. Potassium channels, proliferation and G1 progression. J Membr Biol 1996;154:91–107.
41 Sarugaser R, Lickorish D, Baksh D et al. Human umbilical cord perivascular (HUCPV) cells: A source of mesenchymal progenitors. STEM CELLS 2005;23:220–229.
42 Li GR, Deng XL, Sun H et al. Ion channels in mesenchymal stem cells from rat bone marrow. STEM CELLS 2006;24:1519–1528.
43 Ribera AB, Nguyen DA. Primary sensory neurons express a Shaker-like potassium channel gene. J Neurosci 1993;13:4988–4996.
44 Moran O, Conti F. Properties of the Kv1.1 rat brain potassium channels expressed in mammalian cells: Temperature effects. Biochem Biophys Res Commun 1995;215:915–920.
45 D'Adamo MC, Liu Z, Adelman JP et al. Episodic ataxia type-1 mutations in the hKv1.1 cytoplasmic pore region alter the gating properties of the channel. EMBO J 1998;17:1200–1207.
46 Imbrici P, Cusimano A, D'Adamo MC et al. Functional characterization of an episodic ataxia type-1 mutation occurring in the S1 segment of hKv1.1 channels. Pflugers Arch 2003;446:373–379.
47 Ludwig J, Terlau H, Wunder F et al. Functional expression of a rat homologue of the voltage gated either a go-go potassium channel reveals differences in selectivity and activation kinetics between the Drosophila channel and its mammalian counterpart. EMBO J 1994;13:4451–4458.
48 Robertson GA, Warmke JM, Ganetzky B. Potassium currents expressed from Drosophila and mouse eag cDNAs in Xenopus oocytes. Neuropharmacology 1996;35:841–850.
49 Frings S, Brull N, Dzeja C et al. Characterization of ether-a-go-go channels present in photoreceptors reveals similarity to IKx, a K^{+} current in rod inner segments. J Gen Physiol 1998;111:583–599.
50 Occhiodoro T, Bernheim L, Liu JH et al. Cloning of a human ether-a-go-go potassium channel expressed in myoblasts at the onset of fusion. FEBS Lett 1998;434:177–182.
51 Gryschenko O, Lu ZJ, Fleischmann BK et al. Outwards currents in embryonic stem cell-derived cardiomyocytes. Pflugers Arch 2000;439:798–807.
52 Neusch C, Weishaupt JH, Bahr M. Kir channels in the CNS: Emerging new roles and implications for neurological diseases. Cell Tissue Res 2003;311:131–138.
53 Catterall WA, Goldin AL, Waxman SG. International Union of Pharmacology. XLVII. Nomenclature and structure-function relationships of voltage-gated sodium channels. Pharmacol Rev 2005;57:397–409.
54 Deng XL, Sun HY, Lau CP et al. Properties of ion channels in rabbit mesenchymal stem cells from bone marrow. Biochem Biophys Res Commun 2006;348:301–309.
55 Shirihai O, Merchav S, Attali B et al. K^{+} channel antisense oligodeoxynucleotides inhibit cytokine-induced expansion of human hemopoietic progenitors. Pflugers Arch 1996;431:632–638.
56 Sun W, Buzanska L, Domanska-Janik K et al. Voltage-sensitive and ligand-gated channels in differentiating neural stem-like cells derived from the nonhematopoietic fraction of human umbilical cord blood. STEM CELLS 2005;23:931–945.
57 Weiss ML, Medicetty S, Bledsoe AR et al. Human umbilical cord matrix stem cells: Preliminary characterization and effect of transplantation in a rodent model of Parkinson's disease. STEM CELLS 2006;24:781–792.


See www.StemCells.com for supplemental material available online.